# Response of High-Rise Buildings under Long Period Earthquake Ground Motions

Taiki Saito
Toyohashi University of Technology, Toyohashi, Japan
Email: tsaito@ace.tut.ac.jp

***Abstract*—During the 2011 Great East Japan Earthquake, high-rise buildings in Tokyo, Nagoya and Osaka swayed vigorously and caused damage to non-structural elements such as with the falling of ceiling panels. Those cities are located near deep layers of sediment and such conditions can create long period ground motions of low frequency even when far from the epicenter of an earthquake. These low frequency waves can travel backwards and forwards through the sediment upon meeting hard obstacles like rock, creating ground movement that resonates with tall structures causing them to sway and topple. In this report, the performance of high-rise buildings during the 2011 Great East Japan Earthquake is presented first. Then, the safety of high-rise buildings with long period ground motions in a massive earthquake that may arise in the future is discussed.**

***Index Terms*—high-rise building, long period earthquake ground motion, seismic safety, Great East Japan Earthquake**

## I. Introduction

The impact of long period ground motions on large scale structures was the focus of attention for the first time nationwide with the 2003 Tokachi-Oki Earthquake. Severe damage to oil storage tanks due to fires and the sinking of floating roofs occurred in the city of Tomakomai, which is 220km from the quake epicenter [1]. The cause of the damage was due to the resonance phenomena by matching the liquid sloshing period of a tank and the long period component of the ground motion of around 7sec that was generated in the deep sedimentary plain. In response to this damage, the seismic design spectra for the liquid sloshing of oil storage tanks in the Fire Service legislation in Japan was revised in 2005 by modifying the spectral amplitudes in the long period range. Damage to high-rise buildings due to long period ground motions was also reported for the Mid Niigata Prefecture Earthquake in 2004. Six elevators were damaged and one of eight main cables in an elevator was cut in a 54-story high-rise building in Tokyo, located 250km from the epicenter. Since then, many seismologists have conducted simulations of long period ground motions in the Tokyo, Osaka and Nagoya areas in the event of massive earthquakes, such as the Tokai, Tonankai and Nankai Earthquakes [2]. The intensities of some simulated ground motions are much larger than the level of earthquake ground motion stipulated in the Building Standard Law in Japan. A number of studies have been conducted on the safety of large scale structures relating to long period ground motions. In 2006, the Japan Society of Civil Engineering (JSCE) and the Architectural Institute of Japan (AIJ) submitted "Joint recommendations on earthquake resistance of civil engineering and building structures against long period ground motions caused by subduction earthquakes". AIJ published a book entitled "Structural Response and Performance for Long Period Seismic Ground Motions" in 2007 [3].

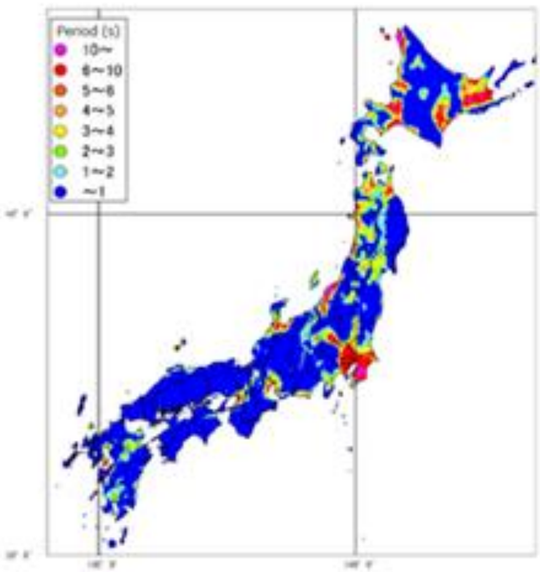


Figure 1. Natural period of deep ground by the central disaster prevention council of the japanese government (2008)

The Central Disaster Prevention Council of the Japanese Government published a map (Fig. 1) on the natural period of deep ground and the predominant period of long period ground motion in 2008. In addition, the Headquarters for Earthquake Research Promotion (HERP) of the Japanese government issued Long Period Ground Motion Hazard Maps in 2009 and 2012. The Ministry of Land, Infrastructure, Transport and Tourism (MLIT) started the Promotional Project for Upgrading the Building Standards in 2009 and one of the primary topics was the "Study on the effect of long period earthquake ground motions to the super-high-rise buildings". In this

Manuscript received December 1, 2015; revised February 1, 2016.



doi: 10.18178/ijscer.5.4.308-314

project, empirical formulas to evaluate long period earthquake ground motions for building design were proposed and a large number of simulation studies were conducted for high-rise and seismically isolated buildings under hypothetical Nankai-Tonankai-Tokai connected earthquakes [4].

## II. Performance of High-Rise Buildings at the 2011 Great East Japan Earthquake

The Building Research Institute (BRI) has been conducting strong motion observation for buildings since 1957. During the 2011 Great East Japan Earthquake, strong motion records were collected at 54 stations located throughout Japan from Hokkaido to the Kansai area (see Fig. 2). Table I shows the list of high-rise buildings under observation and the maximum acceleration values observed in the buildings. Fig. 3 shows the velocity response spectra of the horizontal records at the lowest levels of the high-rise buildings in Miyagi, Tokyo and Osaka cities [5]. The velocity response spectra in Miyagi and Tokyo have a strong component in the wide band period from 0.5 second to 10 seconds. On the other hand, the response spectrum in Osaka has a peak period of 6-7 seconds. This means that the long period ground motion was generated in the deep semimetal soil in the Osaka basin. Since the natural period of Building H is 6 seconds which is close to the dominant period of the ground motion, the response was amplified due to the resonance effect.

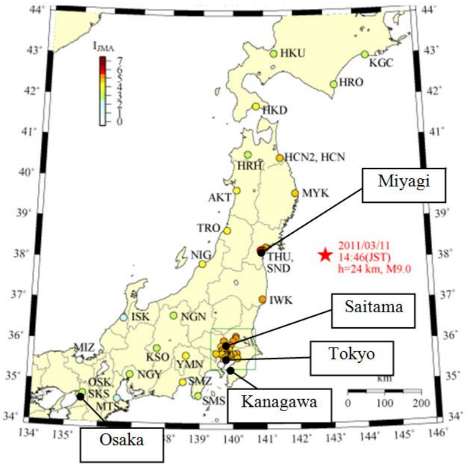


Figure 2. Locations of buildings under earthquake response observation by BRI and name of cities with high-rise buildings

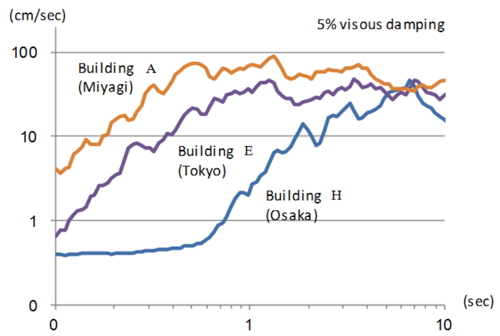


Figure 3. Velocity response spectra in different cities in Japan [5]

TABLE I. List of High-Rise Buildings with Observed Acceleration Records at the 2011 Great East Japan Earthquake (from BRI)

| | Location | Structural Type | Structural system | Floor | $\Delta$ (km) | Location of Sensors | Acc. ($cm/s^2$) | | |
|---|---|---|---|---|---|---|---|---|---|
| | | | | | | | *H1* | *H2* | *V* |
| A | Miyagi | S | Normal | B2F<br>15F | 175 | B2F | 163 | 259 | 147 |
| | | | | | | 15F | 361 | 346 | 543 |
| B | Saitama | S | Control | 26F<br>P2F | 378 | B3F | 74 | 63 | 42 |
| | | | | | | 10FS | 119 | 138 | 62 |
| | | | | | | 10FN | 118 | 155 | 66 |
| | | | | | | P1FS | 248 | 503 | 107 |
| | | | | | | P1FC | 265 | 686 | 185 |
| C | Tokyo | S | Normal | B4F<br>20F<br>P1F | 386 | 01F | 90 | 86 | 45 |
| | | | | | | 20B | 208 | 148 | 173 |
| | | | | | | 19C | 179 | 133 | 130 |
| D | Tokyo | S | Control | B4F<br>21F | 386 | B4F | 75 | 71 | 49 |
| | | | | | | 13F | 137 | 113 | 72 |
| | | | | | | 21F | 121 | 131 | 104 |
| E | Tokyo | RC | Normal | 37F | 385 | 01F | 87 | 98 | 41 |
| | | | | | | 18F | 118 | 141 | 64 |
| | | | | | | 37F | 162 | 198 | 108 |
| F | Kanagawa | S | Normal | B3F<br>23F<br>P1F | 412 | B2F | 60 | - | 30 |
| | | | | | | 23F | 162 | - | 72 |
| G | Osaka | S | Normal | B3F<br>15F | 759 | B3F | 11 | 9 | 5 |
| | | | | | | P3F | 65 | 38 | 7 |
| H | Osaka | S | Normal | 52F<br>P3F | 770 | 01F | 35 | 33 | 80 |
| | | | | | | 18F | 41 | 38 | 61 |
| | | | | | | 38F | 85 | 57 | 18 |
| | | | | | | 52FN | 127 | 88 | 13 |
| | | | | | | 52FS | 129 | 85 | 12 |

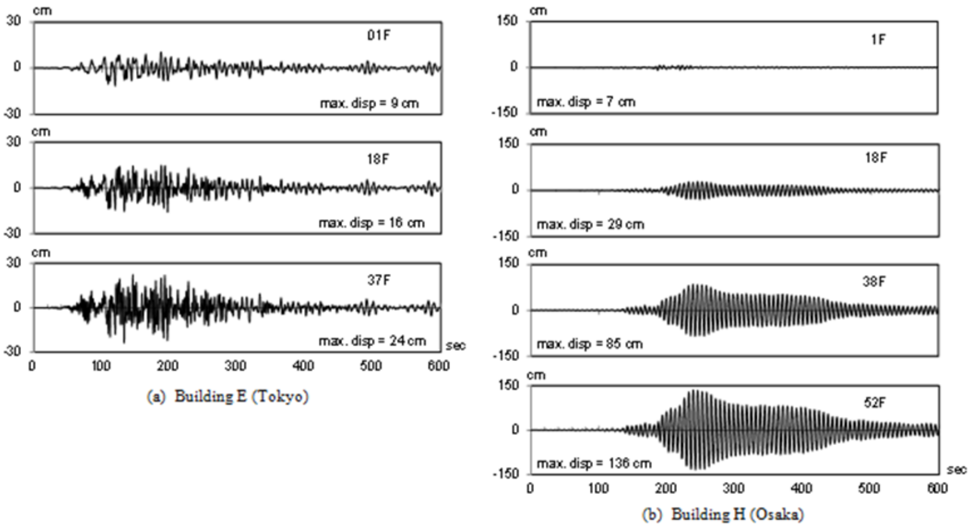


Figure 4. Displacement records of high-rise buildings in Tokyo and Osaka cities (from BRI)

Fig. 4 shows the displacement records observed on different floors of high-rise buildings in Tokyo and Osaka cities. Whereas the maximum displacement at the top floor of Building E in Tokyo, 385 km away from the epicenter, was 24 cm, the large floor movement of 136 cm amplitude was observed at the 52th floor of Building H in Osaka, 770 km away from the epicenter.

In Building H, all 32 lifts stopped and a number of people were trapped in four of them. Damage to non-structural members such as the falling of gypsum boards and ceiling panels were observed extensively.

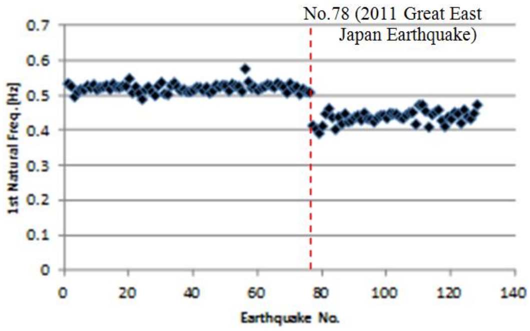


(a) The first natural frequency

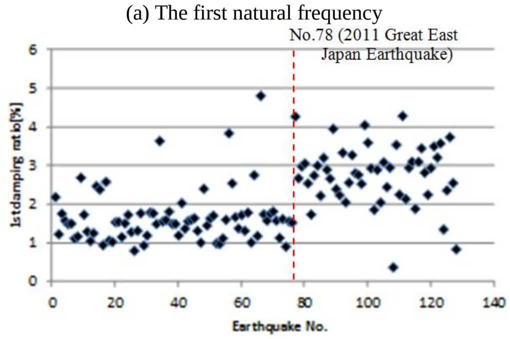


(b) The first mode damping factor

Figure 5. Vibration characteristics of the building E (EW direction)

## III. Valuation of Vibration Characteristics of a High-Rise Building

Using strong motion records captured during the main shock of the 2011 Great East Japan Earthquake, the vibration characteristics of a reinforced concrete high-rise building (Building E) was identified [6]. We obtained continuous strong motion records for this building from May 2007 which has provided us with 130 records including the main shock of the 2011 Great East Japan Earthquake. Using all of these records, system identification was performed to obtain a time series of vibration characteristics such as the first natural frequency and the first mode damping factor of the building as shown in Fig. 5. The first natural frequency declined about 20% and the first mode damping factor increased 2-4% in EW direction of the building after the 2011 Great East Japan Earthquake. This change is considered to be due to the cracks of structural elements that occurred during the main shock. Accordingly, by analyzing the strong motion observation records, it is possible to reveal the damage to the building.

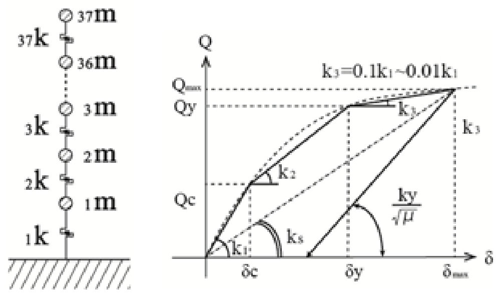


Figure 6. Lumped mass model of the building E

The time history analysis of Building E was conducted using a lumped mass model with a nonlinear shear spring in each story which represents the nonlinear relationship between the story shear force Q and the story drift δ by the tri-linear hysteresis model as shown in Fig. 6. The values of mass, stiffness and the skeleton curve of hysteresis were taken from structural design drawings. The first natural period of this model was calculated as 2.0sec which coincides with the identified natural period before the 2011 event.

The observation record of the main shock of the 2011 Great East Japan Earthquake at the basement (EW direction) was adopted as an input ground motion. The dynamic response of the buildings was calculated using Newmark's β method (β = 0.25) for numerical integration [7]. Regarding the damping matrix, three different damping types were used for comparison:

Type 1(○): $[C]=\alpha[K_0]$

Type 2(●): $[C]=\alpha[K_p]$

Type 3(□): $[C]=\alpha[K_0]+\beta[M]$

Type 1 is the proportional damping to the initial stiffness matrix $[K_0]$, Type 2 is the proportional damping to the nonlinear stiffness matrix $[K_p]$, and Type 3 is Rayleigh damping using the initial stiffness matrix $[K_0]$ and the mass matrix $[M]$.

For each case of damping type, the maximum absolute acceleration and the maximum story drift of each story obtained from the analysis were plotted in Fig. 7. The observed acceleration values obtained by the accelerometers on the 18th floor and the 37th floor are also plotted by the cross mark (×) in the same Figure. Type 2 damping (●) gives relatively good results for the maximum acceleration at the 18th floor. On the other hand, the maximum story drift of Type 2 damping is larger than those of other damping types and reaches around 1/250 in the middle stories. The displacement response on 37th floor in EW direction using Type 2 damping is shown in Fig. 8. The analytical results match quite well with the observed records. The relationship between story shear force and story drift is shown in Fig. 9 for the 1st, 18th and 37th stories. The responses exceeded the crack points in the 1st and 18th stories and stiffness degradation was observed. This result explains the reduction of the natural frequency of the building observed after the 3.11 event as shown in Fig. 5 resulting from minor cracks in structural members.

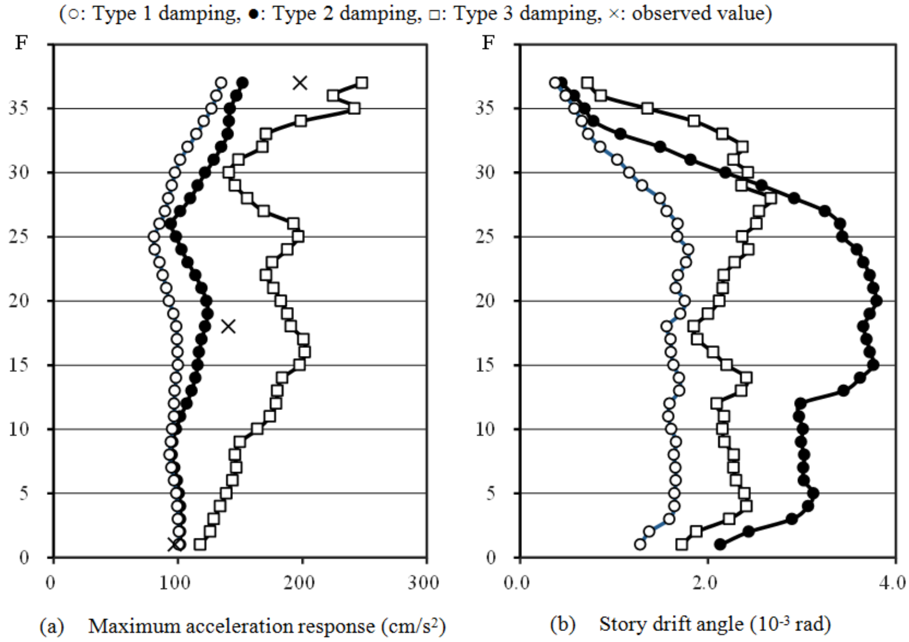


Figure 7. Maximum response of building E (EW direction) with different damping types

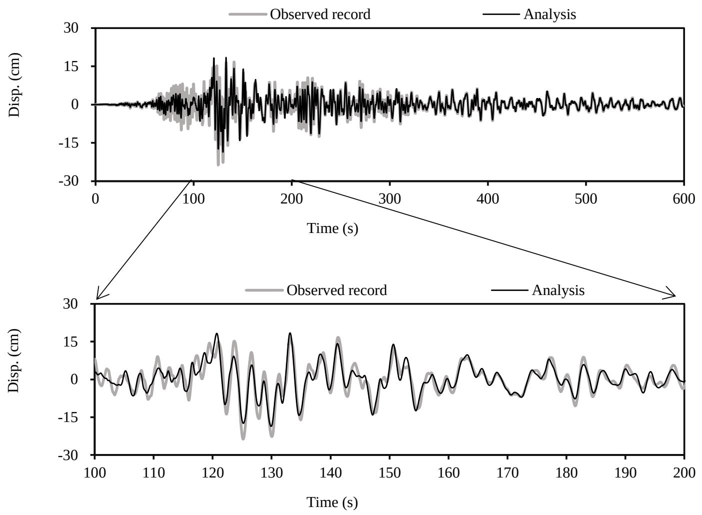


Figure 8. Displacement response of building E (EW direction, $37^{th}$ floor) with type 2 damping

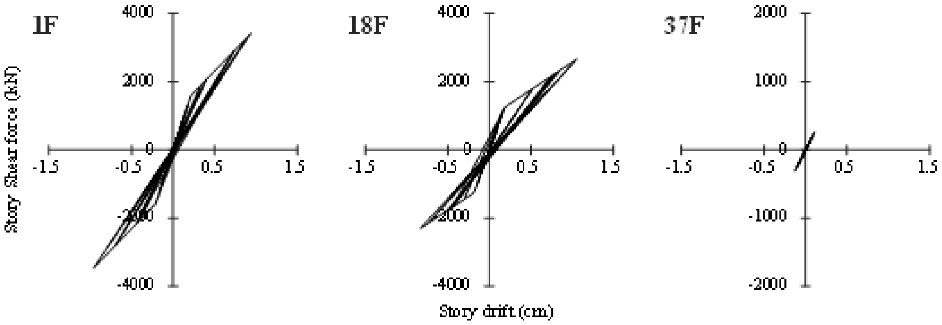


Figure 9. Relationship between story shear and story drift of building E (EW direction) with type 2 damping

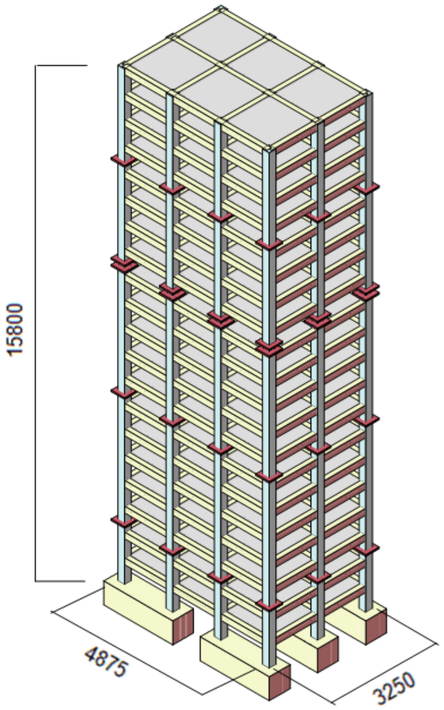


Figure 10. Test specimen of a RC high-rise building

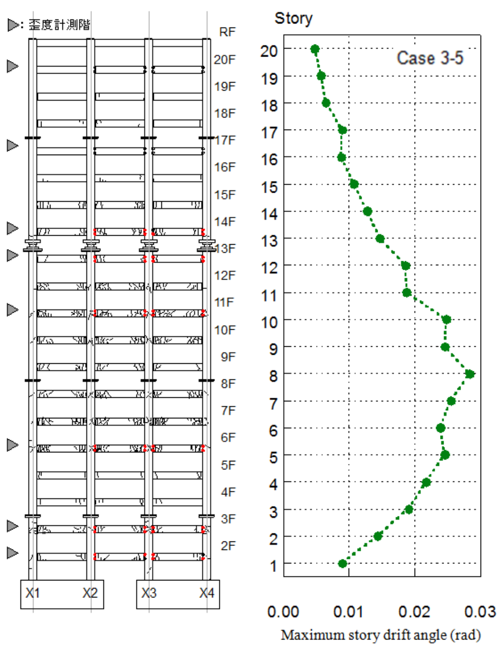


Figure 11. Crack distribution and the maximum story drift

## IV. E-Defense Test of a Reinforced Concrete High-Rise Building under Long Period Ground Earthquake

Shaking table tests were carried out at an E-Defense facility to verify the dynamic response characteristics of a one fourth scaled 20 story high-rise reinforced concrete building specimen under long-period ground motions [8], [9]. Fig. 10 illustrates the elevation of the test specimen. Table II shows the excitation cases. At the final excitation (Case 3-5), the maximum story drift angle was 1/35 at the eighth floor and extensive cracks were observed (Fig. 11). The seismic design regulation of high-rise buildings in Japan requires a limit to the maximum story drift angle of less than 1/100 under the safety level of design earthquake. Therefore, the test results demonstrate the damage to the building is far exceeds the safety level.

TABLE II. Excitation Cases and Maximum Story Drift Obtained from the Test

| | Case | Ratio | Max. Story Drift Angle |
|---|---|---|---|
| Observed record at the 2011 Great East Japan earthquake in Tokyo | 1-5 | 100% | 1/234 |
| | 2-2 | 200% | 1/137 |
| | 2-6 | 300% | 1/86 |
| Simulation wave at Tokai-Tonankai-Nankai earthquake | 3-2 | 150% | 1/64 |
| | 3-5 | 200% | 1/35 |

Nonlinear frame analysis was carried out using STERA_3D to simulate the test results. STERA_3D is integrated computer software for the seismic analysis of steel and reinforced concrete buildings in three dimensional space developed by the author and distributed for free for research and educational purposes [10]. STERA_3D has a visual interface to create a building model and show the results easily and rapidly.

Fig. 12 shows the element models used in STERA_3D. A beam is modelled as a line element with nonlinear flexural springs at both ends. The degrading tri-linear slip model is used for the hysteresis. A column is modelled in a similar manner, and nonlinear interaction between axial force and moment is expressed using axial springs of concrete and steel arranged in sections at both ends.

The purpose of the simulation analysis is to clarify the effect of the following three factors on the results.

1) *Slab contribution to the flexural behavior of a beam*: To consider slab contribution of stiffness and strength to the flexural behavior of a beam, 10% of

the beam length is generally adopted as the effective slab width (see Fig. 13). However, test results suggested the contribution of the full slab width to the flexural strength of the beam.

2) *Slip behavior in the flexural hysteresis of a beam:* Fig. 14 shows the shear-rotation relationship of the 6F beam from the test results. The hysteresis loop contains a slip property.

3) *P-Delta effect*: Since the story drift angle is limited to less than 1/100 in the seismic design regulation of high-rise buildings, the P-Delta effect is generally neglected in the analysis. However, in the test results, the maximum story drift reached 1/35 and it is necessary to examine the effect of P-Delta.

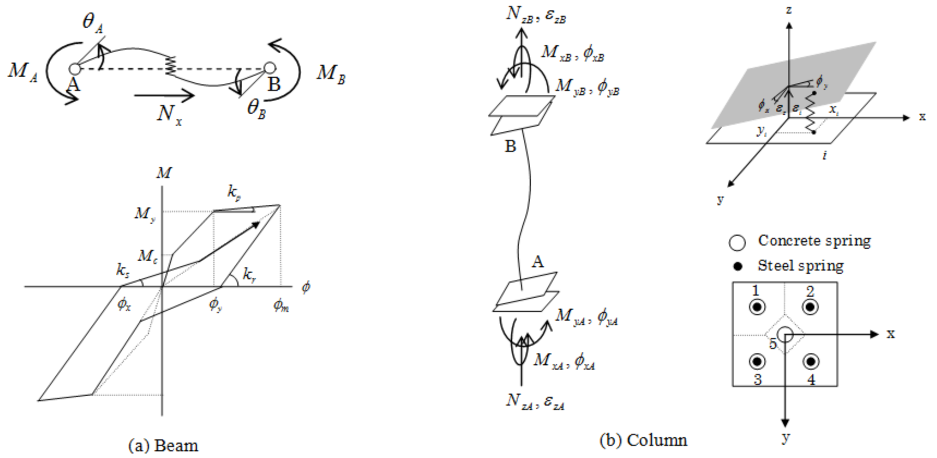


Figure 12. Nonlinear member models used in STERA_3D

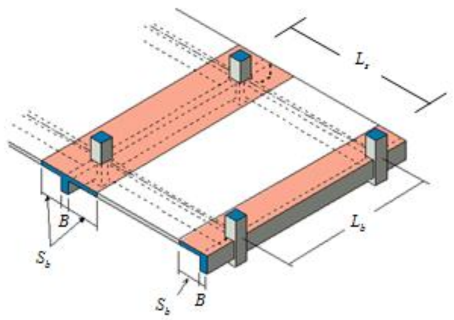

Figure 13. Slab contribution to the flexure of beam

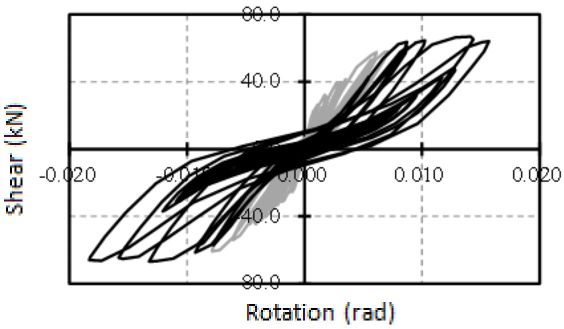


Figure 14. Shear-rotation relationship of 6F beam

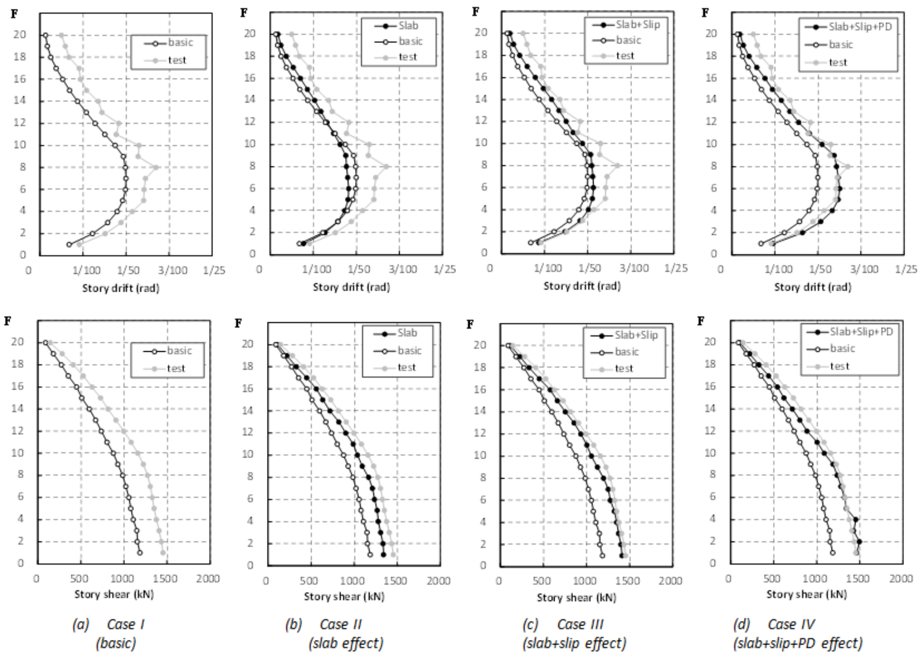


Figure 15. Distributions of the maximum story drift and shear force in each story

Distributions of the maximum story drift and story shear force are compared between test results and analysis results to examine the effect of the above factors in Fig. 15. There are four cases in the analyses.

Analysis Case I is the "basic" case with a slab effect of 10% of beam length, no slip behavior, and no P-Delta effect. As shown in Fig. 15, the results of this case are shown below the test results.

Analysis Case II is the "Slab" case with a full slab effect, no slip behavior, and no P-Delta effect. As shown in Fig. 15, by considering the full slab effect, the story drift becomes smaller than the "basic" case, however, the story shear increases.

Analysis Case III is the "Slab+Slip" case with a full slab effect, slip behavior, and no P-Delta effect. As shown in Fig. 15, by considering slip behavior, the story drift becomes larger than the "basic" case.

Analysis Case IV is the "Slab+Slip+PD" case with a full slab effect, slip behavior, and P-Delta effect. As shown in Fig. 15, by considering all three factors, the analysis results become close to the test results.

## V. Conclusion

The responses of high-rise buildings during the 2011 Great East Japan Earthquake were discussed based on the strong motion observation records. The responses calculated by the time history analysis of a 37-story reinforced concrete high-rise building (Building E) using a lumped mass model matched quite well with the observed records. The analytical also explained the reduction of the natural period of the building after the 2011 event as a result of minor cracks in structural members. Therefore, in the range of minor damage, it was successful to simulate the behavior of a high-rise building by an analytical model.

On the other hand, as demonstrated by the E-defense shaking table test, it was difficult to simulate the behavior of a high-rise building in large nonlinear response range by using a conventional analytical model. From the parametric studies conducted by STERA_3D, it was found that several factors in the analysis such as the slab contribution to the beam flexibility, the slip behavior in the flexural hysteresis of beam elements, and the P-Delta effect must be considered to simulate the large nonlinear response of the high-rise building.

## References


[1] S. Zama, H. Nishi, M. Yamada, and K. Hatayama, "Damage of oil storage tanks caused by liquid sloshing in the 2003 tokachi oki earthquake and revision of design spectra in the long-period range," in *Proc. 14th World Conference of Earthquake Engineering*, Beijing, China, 2008.

[2] Y. Yamamoto and C. Yoshimura, "Long-period ground motion simulation of tokai-tonankai-nankai coupled earthquake based on large-scale 3D FEM," in *Proc. 15th World Conference of Earthquake Engineering*, Lisbon, Portugal, 2012.

[3] Architectural Institute of Japan, *Structural Response and Performance for Long Period Seismic Ground Motions*, 2007.

[4] I. Okawa, T. Satoh, T. Sato, and T. Nishikawa, "An empirical evaluation of long-period earthquake motion for building design," in *Proc. 15th World Conference of Earthquake Engineering*, Lisbon, Portugal, 2012.

[5] T. Saito, K. Morita, T. Kashima, and T. Hasegawa, "Performance of high-rise buildings during the 2011 Great East Japan Earthquake," in *Proc. 15th World Conference of Earthquake Engineering*, Lisbon, Portugal, 2012.

[6] T. Saito, S. Tanaka, and K. Morita, "Identification of vibration characteristics of a reinforced concrete high-rise building damaged due to an earthquake," in *Proc. Japan Concrete Institute*, Takamatsu, Japan, 2014.

[7] A. K. Chopra, *Dynamics of Structures Theory and Applications to Earthquake Engineering*, Prentice Hall, 2007.

[8] K. Sugimoto, H. Katsumata, H. Fukuyama, T. Saito, and T. Kabeyasawa, "Earthquake resistant performance of high-rise reinforced concrete buildings under long-period ground motions," in *Proc. 15th World Conference of Earthquake Engineering*, Lisbon, Portugal, 2012.

[9] K. Sugimoto, *et al*., "Shaking table test of 1/4 scaled 20 story RC building under long period ground motions," in *Proc. Summaries of Technical Papers of Annual Meeting Architectural Institute of Japan*, Sapporo, Japan, 2013.

[10] T. Saito. STERA_3D Software. [Online]. Available: http://www.rc.ace.tut.ac.jp/saito/software-e.html


 